Structures 34 (2021) 1798–1810

Contents lists available at ScienceDirect

Structures

journal homepage: www.elsevier.com/locate/structures

Dynamic behavior of a masonry bell tower subjected to actions caused by bell swinging

Elesban Nochebuena-Mora *, Nuno Mendes, Paulo B. Lourenço, Federica Greco

University of Minho, ISISE, Department of Civil Engineering, Guimarães, Portugal

ARTICLE INFO

Keywords:
Masonry bell tower
Bell swinging
Dynamic forces
Spanish system
Dynamic analysis
Frequency analysis

ABSTRACT

Seismic response of masonry towers has been widely studied, whereas research on their behavior under other dynamic forces is not common. The aim was to study the dynamic effects of bell swinging on a masonry tower, evaluating the response through different approaches. For this purpose, the south tower of the National Palace of Mafra was adopted due to its slenderness and its four swinging bells located at 49 m height. Dynamic identification tests allowed to determine the tower's dynamic properties aimed at calibrating a numerical model. Frequency analyses assessed possible resonance effects by comparing the frequencies of the excitations with those of the tower. Nonlinear dynamic analyses evaluated the response in terms of displacements and cracking, while nonlinear static analyses determined damage patterns assuming different load combinations. Variations of structural stiffness and intensity of the forces were also studied. The results demonstrated that the tower, subjected to bells action, remains within the elastic range with a high safety level. Moreover, crack patterns correspond to local damage, which do not compromise the stability of the structure. Finally, parametric analysis allowed to obtain equivalent static load factors for bells of the Spanish system.

1. Introduction

One of the hardest problems to solve in structural engineering is the response of a building subjected to dynamic actions such as earthquakes, wind, and traffic. The difficulty increases when the studied structure is an ancient construction, since the precise geometry, mechanical properties of the materials, type and efficiency of the connections, among other important parameters, are unknown or difficult to obtain. The response of historical masonry towers has been widely investigated under seismic actions, with the aim of predicting their dynamic behavior and the safety level, for example [1–6]. On the other hand, research addressing their dynamic behavior when subjected to other types of excitations is scarce, including vibrations under service conditions, such as bell swinging. Given their large mass, the bells in motion generate high inertial forces that, in conjunction with certain factors, might damage the masonry in ancient towers. These structures were built before modern structural analysis was developed and, therefore, they were designed using only empirical criteria. Furthermore, the mechanical properties of the materials gradually decrease due to weathering, poor or lack of maintenance, fatigue, and creep. Thus, it is important to assess the safety in order to protect human lives and conserve architectural heritage.

Based on the pattern of oscillation, the bells are classified into three systems: Central European, English, and Spanish. The bells of the Central European system (*alla Romana*) swing through an angle between 55° and 160° [7,8]. In the English system (*Ambrosiano*), the bells are placed in mouth-up position and then released; once they oscillate almost 360°, they stop and shift the direction to oscillate backwards [7,9]. In both systems, the bells are supported by a timber or metallic frame. The bells of the Spanish system rotate always in the same direction describing full circles. They are provided with a wooden counterweight that is placed at the windows of the towers, directly supported by the masonry [7].

In 1913, E.H. Lewis carried out the first analytical work on the behavior of ancient bell tower subjected to bell dynamic forces. By using a device similar to a seismograph, Lewis measured the accelerations of a tower when the bells were swinging. According to the researcher's experiments, the full rotation of a bell can generate horizontal forces up to twice the weight of the bell and vertical forces four times its weight [8].

Müller focused the studies on the Central European system and its impact on the bell towers in Germany in 1960′s. This author recommended to analyze the resonance effect, which may occur if the frequency content of the dynamic forces is close to the fundamental

* Corresponding author at: Elesban Nochebuena-Mora, University of Minho, ISISE, Department of Civil Engineering, Guimarães, Portugal.
E-mail address: enochemora@gmail.com (E. Nochebuena-Mora).

https://doi.org/10.1016/j.istruc.2021.08.066
Received 5 January 2021; Received in revised form 4 August 2021; Accepted 16 August 2021
Available online 9 September 2021

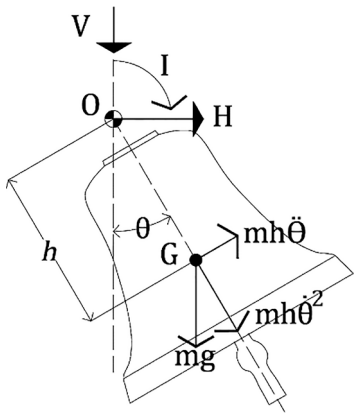

Fig. 1. Dynamic equilibrium of a compound pendulum. Adapted from [12].

frequency of the tower. In 1978, the German code DIN 4178 for the design and construction of new bell towers was created furnishing a simplified method based on Müller's work. The code also contains considerations for the structural assessment, maintenance and restoration of historical towers [8,10]. Bru et al. [11] performed a parametric analysis based on this code to study the behavior of a slender bell tower with Central European system in Italy. The results demonstrated that, under certain combinations of factors (bell location, velocity, and oscillation angle), the bell swinging can cause damage. However, the method can neither predict the safety level of the structure nor the type, location, and severity of the damage.

Heyman and Threlfall developed reliable and straightforward experiments to determine some physical characteristics of the bells that are required to compute the forces, namely moment of inertia and eccentricity (distance between the rotation axis and the gravity center) [9]. From then on, several researchers have carried out studies and published works about the dynamic effects of bell towers with English and Central European systems, mainly in Germany, Italy, and England [12–19]. These works involved in situ measurements of the tower swaying, numerical models used to reproduce the behavior of the buildings, and some mathematical procedures based on the angular position of the bells to estimate the forces.

With regard to the Spanish system of bell ringing, the research was almost non-existent until 2002 [20]. Since this year, Ivorra et al. have published the results of analyses performed in some towers only in Spain. They also compared the characteristics of the three systems (English, Central European, and Spanish), finding significant differences in the magnitude of the dynamic forces and their frequency content [7]. Nevertheless, any of the previous works presents an assessment of the safety levels to estimate the load capacity of the structures for bell swinging.

The present work studies different analysis approaches that can be used for the assessment of the dynamic behavior of masonry towers under bell excitations: frequency analysis, nonlinear dynamic analysis, and nonlinear static analysis. For this purpose, a numerical model of the south tower of the National Palace of Mafra, Portugal, was generated as it is a slender building that houses four swinging bells of the Spanish system located at 49 m height. In 2001, the bells stopped ringing as the safety conditions could not be guaranteed, and given the progressive deterioration, all the bell set was fixed to scaffoldings until its restauration, that was finished in December 2019.

2. Review of the approaches to determine the bell forces

A bell swinging is considered as a compound pendulum when its center of mass G is not coincident with the pivot point or rotation axis O, as depicted in Fig. 1 [21]. Thus, the dynamic forces depend on its mass m, eccentricity h (distance between point O and G), initial angular position α, and initial angular velocity ω_α, neglecting friction influence. Bennati et al. [12] proposed an experimental test to measure the mass in terms of a tensile force on a cable that sustains the bell in an out of balance position. The eccentricity and moment of inertia can be obtained using the methodology presented by Heyman and Threlfall [9] or using a dynamometer [8]. Finally, initial angular velocity is a variable parameter that depends on the force applied to the bell for initiating the motion.

Table 1
Multiplication factors to determine the maximum dynamic forces based on the weight of the bell.

Reference	Bell ringing system	V_{max}	H_{max}
Whitechapel Bell Foundry in London[a]	English	4.5	2.5
Lewis, Heyman and Threlfall [9]	English	4	2
Manuale dell'Achitetto[b]	English	1.5	0.25
Manuale dell'Achitetto[b]	Central European	3.1	1.55

[a] Referenced in [8]
[b] Referenced in [12]

2.1. Empirical approach

Empirical approaches are simple formulations that only consider the weight of the bell using a multiplier factor to obtain maximum equivalent static forces. For example, Whitechapel Bell Foundry in London proposes the factors 2.5 and 4.5 for the maximum horizontal and vertical load, respectively (referenced in [8]). According to Heyman and Threlfall [9], the vertical force is approximately four times the weight and the horizontal load is two times. *Manuale dell'Architetto* (referenced in [12]) distinguishes between two types of systems (English and Central European) and suggests different factors for each (Table 1). These formulations are conservative, do not consider the eccentricity, angular velocity, and initial position, and provide only maximum values of forces.

2.2. Dynamic forces in terms of angular displacement

Wilson and Selby [21] developed simple and accurate equations to calculate the dynamic forces as function of the angular displacement. These equations introduce an inertial form factor c in terms of the eccentricity h and the radius of gyration r (Eq. (1)). A parameter p is also used to consider the initial velocity ω_α and initial position α (Eq. (2)). The values for eccentricity, period τ, and moment of inertia I, which is related to the radius of gyration through Eq. (3), are determined by experimental tests [9].

$$c = \frac{h^2}{h^2 + r^2} \tag{1}$$

$$p = \cos\alpha + \frac{\omega_\alpha^2 \tau^2}{8\pi^2} \tag{2}$$

$$I = m(r^2 + h^2) \tag{3}$$

Then, the vertical V and horizontal H forces are calculated as function of the angular position θ, where m is the mass of the system and g is the acceleration of gravity:

$$V = mgc\left(\frac{1-c}{c} + 3cos^2\theta - 2p\cos\theta\right) \tag{4}$$

$$H = mgc\sin\theta(3\cos\theta - 2p) \tag{5}$$

2.3. Dynamic forces as function of time

The time-varying forces involve the calculation of the angular position, angular velocity, and angular acceleration at any given time. The

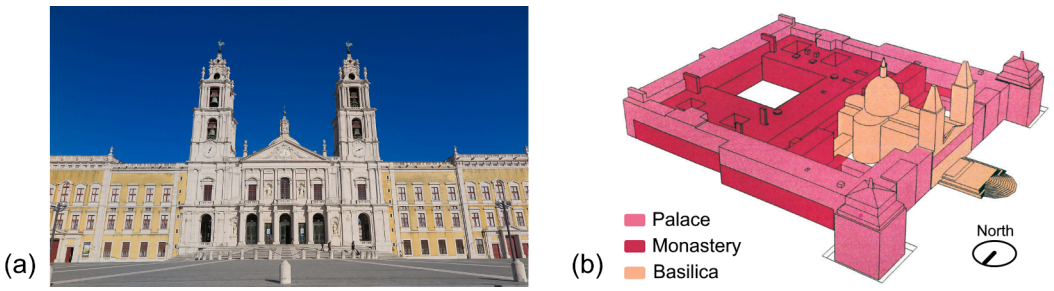

Fig. 2. (a) Façade of the Basilica (image by authors) (b) Distribution of functional spaces [30].

linear equation for simple harmonic motion is appropriate for small amplitudes (θ less than 7°) giving an error less than 0.1%. It assumes that sin θ ≈ θ, which yields to a solution with a sinusoidal function of time. Nevertheless, this strategy is not accurate to characterize the behavior of the bells, since the error becomes higher as the amplitude increases and approaches to 180° [22,23]. For large angles, and neglecting damping and friction effects, nonlinear differential equation Eq. (6) describes the motion of a compound pendulum in terms of mechanical energy:

$$E = \frac{1}{2} I\dot{\theta}^2 + mgh(1 - \sin\theta) \tag{6}$$

where $\dot{\theta}$ is the angular velocity, I is the moment of inertia, the term $I\dot{\theta}^2/2$ is the kinetic energy, and the term $mgh(1 - \sin\theta)$ is the potential energy at any given point of the oscillation. When the total energy E is higher than $2mgh$, the pendulum rotates around the axis in a unidirectional periodic motion, describing full circles like the Spanish bells. Based on the work presented by Lima [22] for the solution of a simple pendulum, it was possible to deduce the analytical solution for a compound pendulum by including the moment of inertia into the equations. The final expression to calculate the angular displacement as function of time of a compound pendulum is:

$$\theta(t) - 2n\pi = \begin{cases} 2\arcsin[sn(\omega(t - nT); k)], nT \le t < \left(n + \frac{1}{2}T\right) \\ 2\pi - 2\arcsin[sn(\omega(t - nT); k)], \left(n + \frac{1}{2}\right)T \le t < (n + t)T \end{cases} \tag{7}$$

where n is the number of turns completed at time t, sn is the elliptic sine, T is the period, $\omega = \sqrt{E/2I}$, and $k \equiv \sqrt{(2mgh/E)}$. The first line of the equation determines the angular position in the first half of the period of every rotation or cycle, while the second line gives the angular position in the second half. Once the angular displacements are obtained, angular velocity and angular acceleration are calculated through the first and second derivative. Finally, the time-varying horizontal and vertical forces are given by the following equations [12]:

$$H(t) = mh\left[\dot{\theta}^2(t)sin\theta(t) - \ddot{\theta}(t)cos\theta(t)\right] \tag{8}$$

$$V(t) = -mg - mh\left[\dot{\theta}^2(t)cos\theta(t) + \ddot{\theta}(t)sin\theta(t)\right] \tag{9}$$

Other strategies for the solution of the nonlinear differential equation Eq. (6) use numerical methods, such as the well-known Taylor series [24], Fourier series [23,25] or Runge-Kutta method [26,27], which solve the problem by approximation to the exact solution with accuracy and efficiency.

3. Description of the building

The Royal Building of Mafra, also known as National Palace of Mafra (Fig. 2a), is a Portuguese building of the 18th century located 30 km in the northwest of Lisbon. The complex, which is the most important work of Baroque-style in the country, was built during the reign of João V and designed by the architect Johann Friederich Ludwing [28] based on buildings of Rome. The building was conceived as a Franciscan monastery, containing a Basilica and a residence for the royal family [29]. In

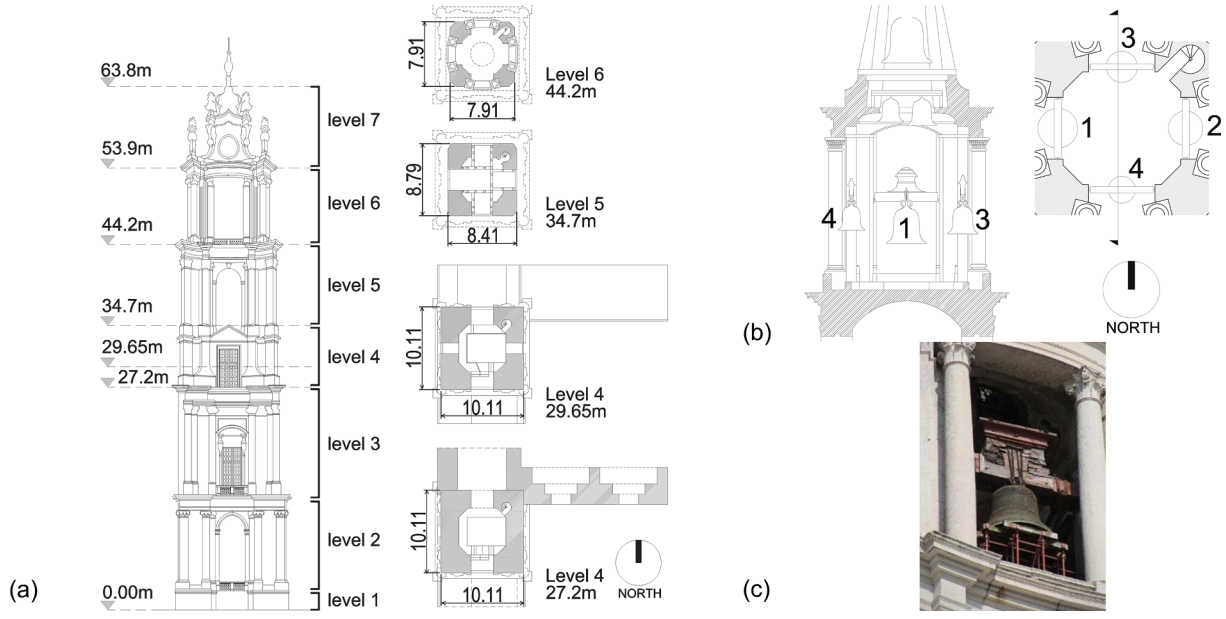

Fig. 3. (a) Façade and plans of the upper levels of the south tower (approximate dimensions) (b) location of the bells on level 6 and (c) the heaviest liturgical bell (bell 1).

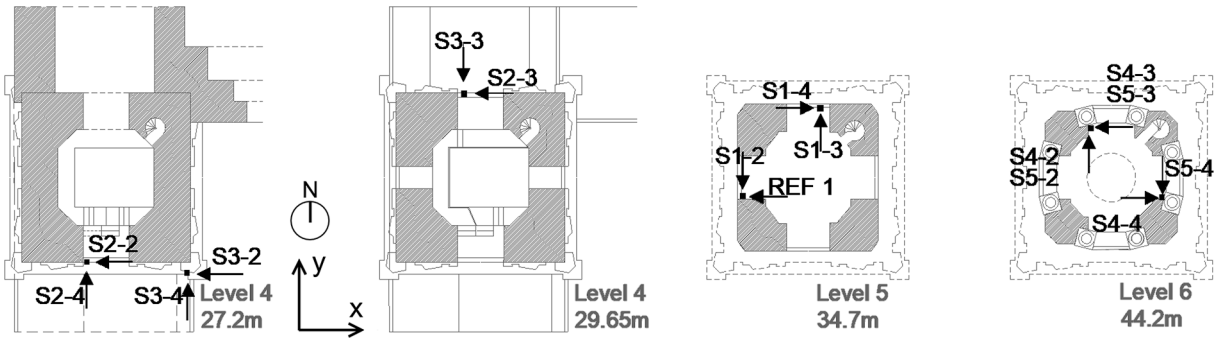

Fig. 4. Setup configurations for dynamic identification test. Setup number: S1-, S2-, S3-, S4-, S5-. Accelerometer number: 2, 3, 4. Reference accelerometer: REF 1.

2019, it was included in the UNESCO World Heritage List as the architectural and material characteristics of the complex have remained virtually intact over time [30].

Both towers have a squared plan and comprise seven levels that reach an approximate height of 63.80 m. On each level, the vertical bearing elements consists of four piers with a large cross-section that support the masonry domes, lintels and semi-circular arches. The three lower levels have the same size in plan, whereas the fourth, fifth and sixth levels present reduction of the plan dimensions in elevation. The seventh level consists of a masonry dome with pyramidal-like shape (Fig. 3a).

3.1. The south bell tower and its bells

The first three levels of the south bell tower serve as passageways to connect the southern chambers with the northern side of the Palace. There are 60 bells in the tower divided into three types: the bells of the carillon, the liturgical bells, and the clock bells. The forth level contains the clock mechanism and the carillon machinery while the fifth floor houses the carillon. This musical instrument comprises 53 fixed bells of several size; 52 of them are attached to a robust timber structure rested on the floor, whereas the heaviest bell is directly anchored to the jambs of the western opening by means of a wooden counterweight.

On the sixth level, there are four liturgical bells of different masses, each one located at the frame of the openings. The bells have a wooden counterweight that is supported on the masonry through rolling bearings, allowing the full rotation of the bells (Fig. 3b and c) and therefore, the only bells capable of swinging. Given their characteristics, the liturgical bells correspond to the Spanish system, i.e. they rotate 360° in only one direction.

The three clock bells, also with different diameter, were attached to steel beams on the seventh level and are rung by a mechanism connected to the clock of the fourth level. In conclusion, the carillon and the clock bells (56 bells) represent vertical static loads since they are completely fixed, whereas the weight of the four liturgical bells becomes dynamic forces when they are in motion.

3.2. Dynamic identification test

The dynamic behavior of the south bell tower was identified from ambient tests aiming at determining the natural frequencies and the mode shapes. The equipment used for the test consisted of piezoelectric accelerometers (PCB Piezotronics) with a sensitivity of 10 V/g, measurement range ± 0.5 g, and a frequency range between 0.15 and 1000 Hz. The signals, with a sampling frequency of 200 Hz, were gathered by an acquisition system of 24-bit resolution and processed using ARTeMIS software [31] with the Enhanced Frequency Decomposition Domain Method (EFDD) [32]. Five setups were performed employing four accelerometers, one of the sensors always placed on level 5 (labeled as REF 1 in Fig. 4) and used as a reference in all the setups. The monitoring points were located on levels 4, 5, and 6. The first setup was recorded on level 5 (labeled as S1), second and third setup (S2 and S3, respectively) were deployed on level 4 at a different height, and fourth and fifth setup (S4 and S5) were located on level 6. In order to identify possible torsional modes of the tower, the accelerometers (2, 3, 4 and REF 1) were disposed on diagonal, close to the windows, and orthogonally orientated to measure accelerations in X and Y axes. Fig. 4 presents the setup configuration, where the arrows indicate the direction of the measurements.

The test allowed to estimate the first two modes of vibration, which in general have the highest contribution for the dynamic behavior (high values of mass participation), since they represent global mode shapes that involve the entire mass of the tower. Mode 1, with a frequency of 2.85 Hz, corresponds to a simple bending of the whole structure in east–west axis (X direction). Mode 2 has a frequency of 5.99 Hz and, due the constraining effect of the adjacent buildings, it is associated to a

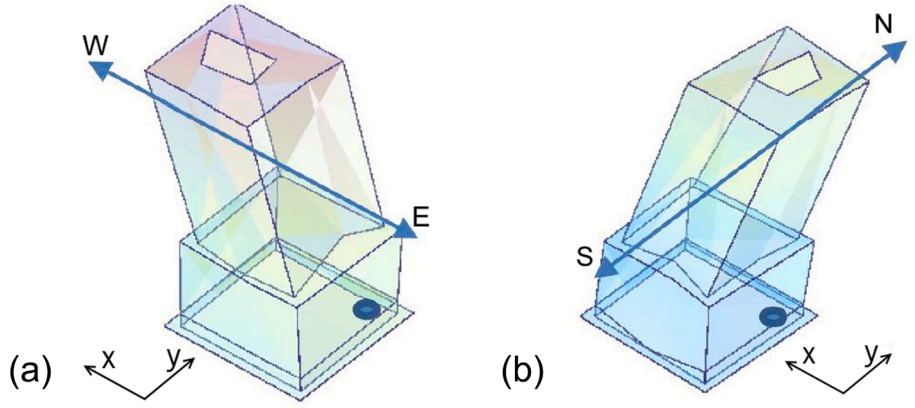

Fig. 5. Mode shapes determined through dynamic identification tests: (a) Mode 1 = 2.85 Hz (X direction), and (b) Mode 2 = 5.99 Hz (Y direction).

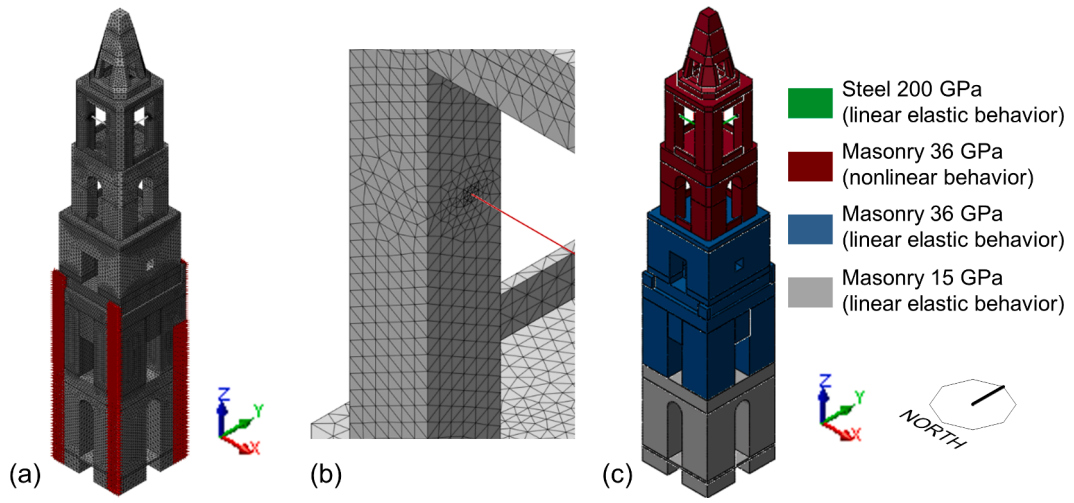

Fig. 6. (a) FEM model with the spring elements in red, (b) reduction of the element size around the plates, and (c) distribution of materials. (For interpretation of the references to colour in this figure legend, the reader is referred to the web version of this article.)

simple symmetrical curvature of the upper levels in north–south axis (Y direction) (Fig. 5).

4. Finite element model

4.1. Geometry and mesh

A 3D model of the south tower was built using Midas FX + for DIANA software [33]. The model considered only the seven levels of the structure with a simplified geometry that neglected architectural details like decoration. The influence of the Basilica and Palace was taken into account by placing spring elements on the north, south, and east façades of the three lowest levels, as shown in red in Fig. 6a. Beams anchored to the masonry were adopted to apply the dead load of the heaviest bell of the carillon (on level 5) and the largest clock bell (on level 7). Four beams placed at the openings of level 6 represented the counterweights of the swinging bells. Steel plates of 0.30 × 0.30 × 0.01 m at the ends of each beam simulated the connections between counterweights and masonry. Other two steel plates with the same dimensions were placed to apply the vertical load of two clock bells on level 7.

The numerical model was based on the Finite Element Method (FEM) and comprised three types of elements: solid elements for masonry, shell for plates and beams for counterweights. The size of the elements ranged between 0.30 and 0.50 m, while a more refined mesh, of element size of 0.15 m, was created around the plates (Fig. 6b). In general, the interface soil-foundation presents high stiffness under low vibration levels for service conditions. Therefore, the nodes at the base of the model were pinned, providing a fixed boundary condition. In addition, one-node spring elements were placed on three façades to provide stiffness at the connection with the Basilica and Palace.

4.2. Materials and FEM model calibration

The whole tower was built with limestone units of good quality and laid in thin mortar joints. The ashlar stones of the first two levels are small, whereas the units of the other five levels are significantly larger (around 1.5 to 1.9 m high). The uniform thickness and regularity of the joints provide the ashlar masonry with strength and sturdiness. Such factors allow to assume the masonry as a homogeneous isotropic material. Based on [13], linear elastic behavior of masonry was adopted for the levels of the tower where no damage is expected (levels 1 to 4). On the other hand, nonlinear response of masonry was considered in the structural elements where cracks may develop as local damage (levels 5 to 7). A total rotating strain model was adopted for the masonry, which defines the nonlinear compressive and tensile behavior of the material. This constitutive model is able to describe reliably the softening and cracking phase in masonry [34]. Crack propagation is determined by the shape of the stress–strain diagrams, in which the fracture energy G_f^I for tension and G_c for compression are represented by the area under the curve. The tensile softening is defined by an exponential curve, and compression hardening and softening are given by a parabolic function [35]. Values for density, and compression and tensile strength were taken from the Italian code [36], while the fracture energies for tension G_f^I and for compression G_c were calculated according to [37,38].

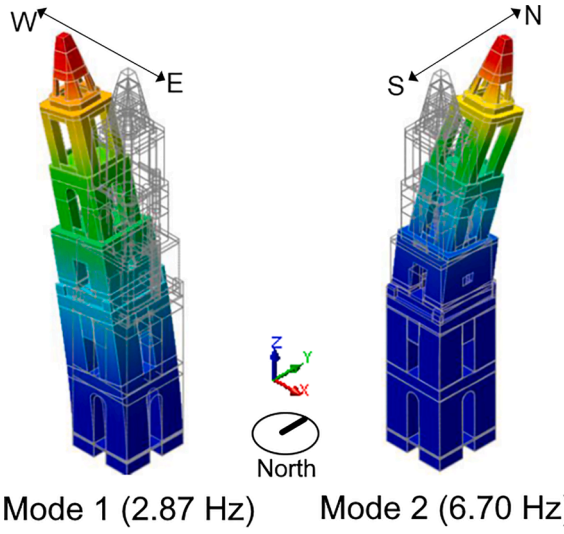

Fig. 7. Eigenvalue analysis: mode shapes of the first two modes obtained from the updated numerical model.

Eigenvalue analysis was first performed on the FEM model, aiming at estimating the natural frequencies and mode shapes. Due to the lack of information regarding the actual mechanical properties of the materials, an initial value of 3.2 GPa for the elastic modulus of the masonry was also taken from the Italian code [36]. Since the lowest modes usually have the major contribution to the dynamic response of the building [39], only the frequencies of the two first modes were used to calibrate the FEM model (Fig. 7). Regarding the mode shapes, a qualitative comparison was done to verify that the numerical mode shapes

Table 2
Updated mechanical properties of the materials after model calibration.

Material	Density (kg/m^3)	Poisson's ratio	Young's modulus (GPa)	Compressive strength (MPa)	Compressive fracture energy (kN/m)	Tensile strength (MPa)	Tensile fracture energy (kN/m)
Stone masonry (levels 1 and 2)	2200	0.20	15				
Stone masonry (levels 3 and 4)	2200	0.20	36				
Stone masonry (levels 5 to 7)	2200	0.20	36	8.00	4.80	0.30	0.05
Steel	7800	0.26	200				

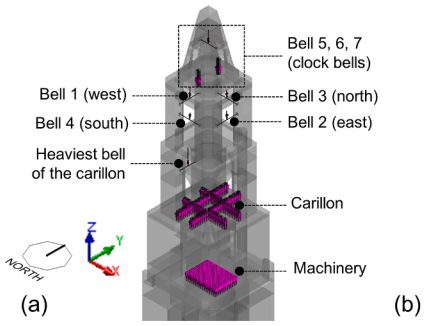

(b)

Bell	Location	Diameter (mm)	Mass (kg)	Bell mass + counterweight mass (kg)	Weight (kN)
Bell 1	Level 6 (West)	1985	4449.52	7119.24	69.84
Bell 2	Level 6 (East)	1720	2887.75	4620.40	45.33
Bell 3	Level 6 (North)	1560	2150.93	3441.49	33.76
Bell 4	Level 6 (South)	1350	1390.55	2224.88	21.83
Bell 5	Level 7	2530	9900.00		97.12
Bell 6	Level 7	1570	2192.80		21.51
Bell 7	Level 7	1380	1485.89		14.58

Fig. 8. (a) Distribution of the dead loads and (b) weight of the bells of levels 6 and 7.

correspond to those of experimental test, namely, simple bending of the whole structure in X direction for Mode 1 and simple bending of the four upper levels in Y direction for Mode 2. The outcomes were compared with the results of the dynamic identification test, obtaining an initial average error of about 51% between experimental and numerical frequencies, specifically, the model presented a frequency of 1.28 Hz for Mode 1, representing an error of 55% in relation to the experimental outcomes, while Mode 2 had a frequency of 3.15 Hz, with an error of 47%. Since the updating process was manually performed, few sensitive parameters were considered. Thus, the calibration of the numerical model was conducted by adjusting only the elastic moduli of the masonry (taking into account the different sizes of the ashlar units) and the stiffness of the springs (modelled as linear with constant stiffness). For the properties of the masonry, lower and upper limits were defined according to the available literature. Regarding the springs, an equivalent normal stiffness induced by the contiguous walls was estimated. It is noted that, although the spring constraints is a relevant variable, it is the least sensitive parameter [40]. After the calibration, performed by using an optimization algorithm with an objective function equal to the difference between numerical and experimental frequencies, the average error decreased to 1.27%. As expected, the results showed high values for the elastic modulus [41] of the masonry given the large size of the blocks on the upper levels (nearly a monolithic structure), and the good quality of construction and material. Regarding the springs, the calibrated normal stiffness is equal to 2000 kN/m.

Table 2 presents the final mechanical properties of the materials after calibration of the numerical model. Young's modulus of the stone is within the range presented in limestone samples tested in laboratory by [41]. Regarding beams and plates, steel with elastic properties was adopted (Fig. 6c).

5. Loads

5.1. Static loads

Besides the self-weight of the structure, the loads considered as static actions are the weight of the clock, machinery, carillon, and clock bells. The mass of the four liturgical bells was accounted as static loads when they are at rest and as dynamic forces when they are swinging. The mass of the clock and machinery (83,428 kg [42]) was applied as a vertical pressure equal to 5.8 kN/m^2 on level 4. Regarding the carillon, a timber structure supports 52 bells summing a total weight of 1,064 kN, which was applied as a vertical pressure of 127.5 kN/m^2. The mass of the largest bell of the carillon (9,640 kg) was multiplied by a factor of 1.6 [8] to account the wooden counterweight. The resulting weight (151.31 kN) was applied as a concentrated load at the center of the beam. The weight of the heaviest bell (hour bell) on level 7 (97.12 kN) [42] was also placed at the center of the beam.

There is no information about the mass of the liturgical bells and two of the clock bells. Since it was not possible to perform any experimental test, their weights were calculated by means of an extrapolation based on the diameter and mass of the other bells (carillon and hour bell). The masses of the four liturgical bells were then increased by 60% to include their counterweights (factor of 1.6 [8]). These weights were applied as a concentrated load at the center of the beams on level 6. Fig. 8 depicts the location of the loads and summarizes the weight of the bells on level 6 and level 7.

5.2. Dynamic loads

Eccentricity, moment of inertia, and initial angular velocity of the

Table 3
Characteristic of the liturgical bells on level 6.

Bell	Location	Weight (kN)	Eccentricity (m)	Moment of inertia (kg m^2)	Initial angular velocity (rad/s)
Bell 1	Level 6 (West)	69.84	0.015	24.92	1.25
Bell 2	Level 6 (East)	45.33	0.019	21.91	1.44
Bell 3	Level 6 (North)	33.76	0.022	19.65	1.59
Bell 4	Level 6 (South)	14.58	0.027	16.10	1.84

Table 4
Absolut maximum dynamic forces produced by the bells.

Bell	As a function of angular position				As a function of time Analytical solution				As a function of time Numerical solution (Runge-Kutta method)			
	H_{max} (kN)	V_{max} (kN)	a	b	H_{max} (kN)	V_{max} (kN)	a	b	H_{max} (kN)	V_{max} (kN)	a	b
Bell 1 (West)	13.40	87.40	0.19	1.25	14.03	87.93	0.20	1.26	13.90	87.97	0.20	1.26
Bell 2 (East)	10.13	58.60	0.22	1.29	10.79	59.29	0.24	1.31	10.73	59.31	0.24	1.31
Bell 3 (North)	8.56	44.97	0.25	1.33	8.99	45.38	0.27	1.34	8.93	45.40	0.27	1.35
Bell 4 (South)	6.93	30.90	0.32	1.42	6.97	30.81	0.32	1.41	6.91	30.83	0.32	1.41

a Ratio of maximum horizontal force to the weight of the bell;
b Ratio of maximum vertical force to the weight of the bell.

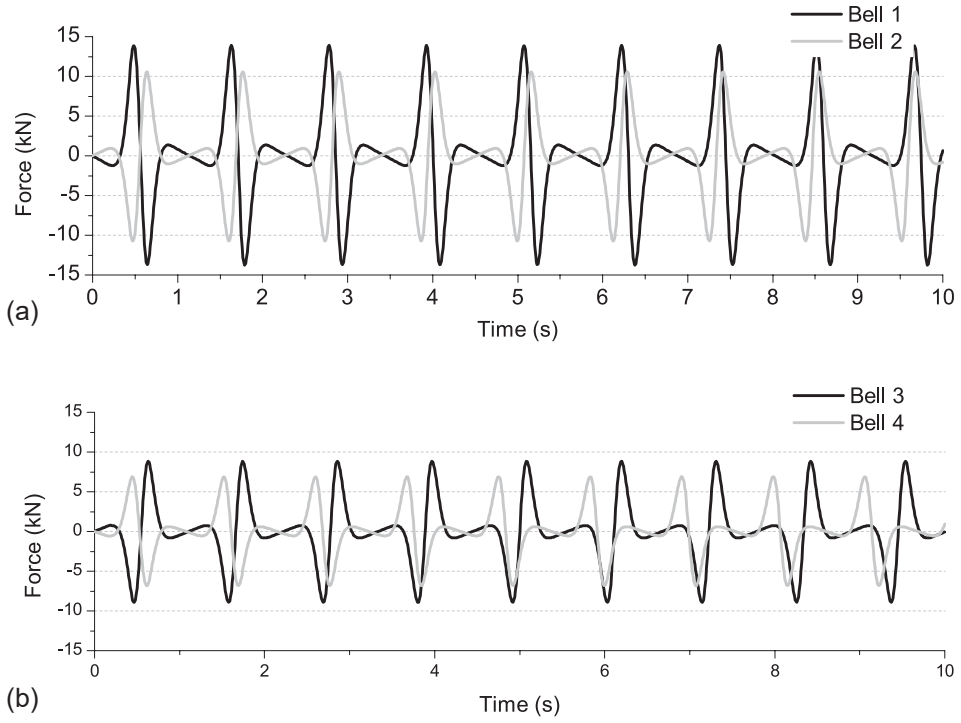

Fig. 9. Horizontal forces as function of time produced by (a) bells 1 and 2 (X direction), and (b) bells 3 and 4 (Y direction).

liturgical bells were determined by extrapolating the data presented in Ivorra et al. [7], where five bells with different masses of the Spanish system were tested in the laboratory. Table 3 presents the characteristics assumed for the liturgical bells.

The forces caused by swinging of the bells were calculated as function of time through the analytical solution given by Eq. (7) and the numerical Runge-Kutta method (RK2), implementing a routine in Matlab R2014 software [43] to solve the second order differential equations. Additionally, the maximum horizontal and vertical forces were also calculated as function of angular position using Eq. (4) and Eq. (5). Table 4 presents the absolute maximum dynamic forces of the four liturgical bells and the ratio of maximum forces to bell weight (columns a and b), i.e., the multiplier factor to calculate the maximum horizontal and vertical equivalent static forces. Notice that the values approximate those proposed by the *Manuale dell'Architetto* for the English system (see Table 1).

As can be noticed, the time-varying values are quite similar, whereas the results obtained as function of angular position are slightly lower. To determine the direction of the dynamic forces, it is assumed that the bell ringer impulses the bell from the inside of the tower, so that the rotation of the bells occurs outwards. Thus, the eastern and northern bell rotate in a positive direction, whereas western and southern bell swing in negative direction. Fig. 9 shows the plotted horizontal forces as function of time produced by the four bells. The dynamic forces (vertical and horizontal components) are assumed as time-varying concentrated loads applied at the center of the beams on level 6.

6. Assessment based on frequencies

Assessment based on frequencies is a simple approach included in the German code [10] that compares the frequency content of the dynamic actions with the fundamental frequency of the tower, aiming at identifying possible resonance effects. The frequency spectrum of the dynamic actions was estimated through the Fast Fourier Transform (FFT), algorithm implemented in Matlab R2014a software [43]. Each peak represents a harmonic and its contribution to the complex signal is given by the amplitude. Fig. 10 depicts the results of the frequency decomposition for the horizontal forces of each bell which correspond to the first, third, fifth, seventh, and ninth harmonic. The second, forth, sixth, and eigth harmonics are related to the vertical forces. As the vertical stiffness of the bell tower is much higher than its bending stiffness, the frequency decomposition of the vertical forces was excluded from the analysis.

According to the literature [20], the frequency of the first harmonic is predominant in bells of the Spanish system. However, given the high mass and the low initial angular velocity, the four bells generate dynamic forces with predominant frequencies associated to the third

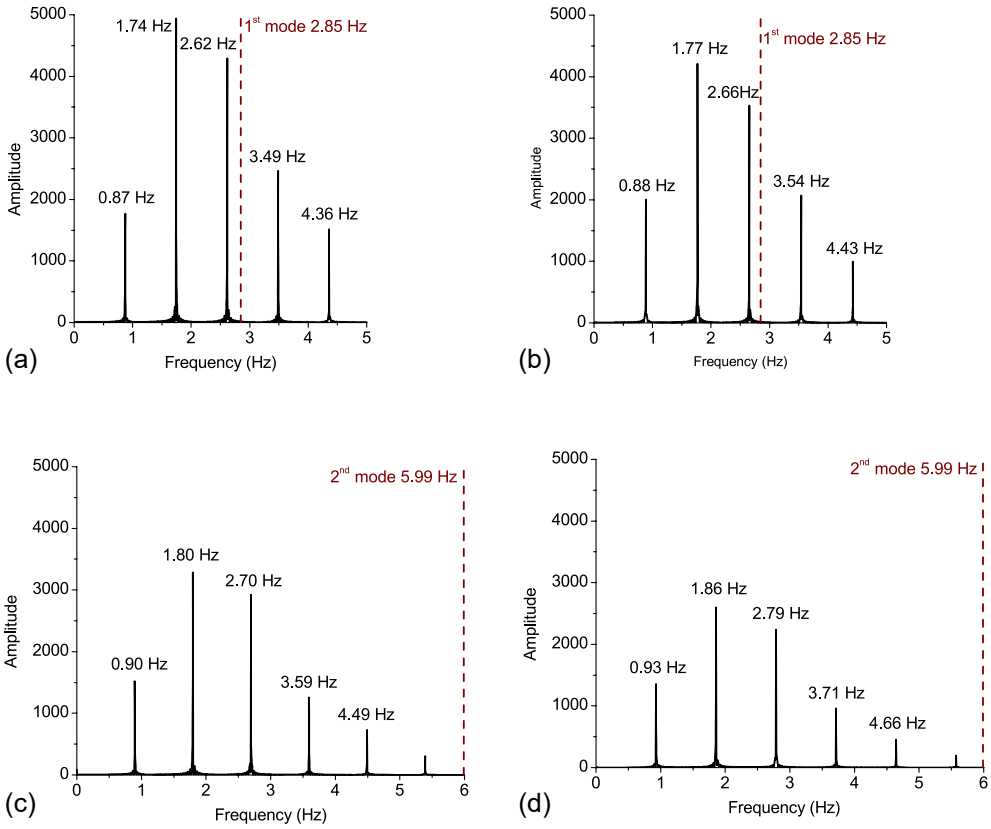

Fig. 10. Frequency spectrum of the horizontal dynamic forces of (a) bell 1, (b) bell 2, (c) bell 3, and (d) bell 4.

Table 5
Fundamental frequencies of the tower and frequencies of the horizontal dynamic forces.

Bell	Frequencies of the bell tower		Frequencies of the horizontal dynamic forces		Difference between frequencies (%)
	Mode 1 (Hz)	Mode 2 (Hz)	1st Harmonic (Hz)	3rd Harmonic[a] (Hz)	
Bell 1 (West)	2.85		0.87	1.74	39
Bell 2 (East)	2.85		0.88	1.77	38
Bell 3 (North)		5.99	0.90	1.80	70
Bell 4 (South)		5.99	0.93	1.86	69

[a] Predominant harmonic.

Table 6
Fundamental frequencies of the tower and frequencies of the horizontal dynamic forces increasing the initial angular velocity to 4.90 rad/s for bell 1 and 3.97 rad/s for bell 2.

Bell	Frequency of the bell tower	Frequencies of the horizontal dynamic forces (input signal)			Difference between frequencies (%)
	Frequency Mode 1 (Hz)	1st harmonic (Hz)	3rd harmonic[a] (Hz)	5th harmonic (Hz)	
Bell 1 (west)	2.85	1.40	2.80	4.20	1.8
Bell 2 (east)	2.85	1.25	2.51	3.77	12

[a] Predominant harmonic.

harmonic. The German Code DIN4178 [10] is the only known standard addressing the design of bell towers in Europe. According to it, the natural frequency of the existing towers must be at least 10% distant from the predominant frequency of the horizontal dynamic forces. Since the rotation of bell 1 and bell 2 occurs in east–west axis (X direction), their frequencies were compared with the first mode (2.85 Hz), whereas the frequencies of bell 3 and bell 4 were compared with the second mode (Y direction) (5.99 Hz). The results demonstrated that there is no interaction between the tower and the bells as frequencies of the dynamic actions are quite distant from the structure's fundamental frequencies in both directions (Table 5).

The tower is more flexible and vulnerable in the X direction (mode 1), which has the lowest frequency, thus the dynamic forces are more likely to achieve such value if the velocity of the bells is increased. Initial angular velocity for bell 1 was set to 4.90 rad/s reaching a frequency of 2.80 Hz (third harmonic), and for bell 2 it was increased to 3.97 rad/s, achieving a value of 2.51 Hz (third harmonic). Table 6 presents the comparison between frequencies, showing that only bell 1 may cause resonance effects on the tower.

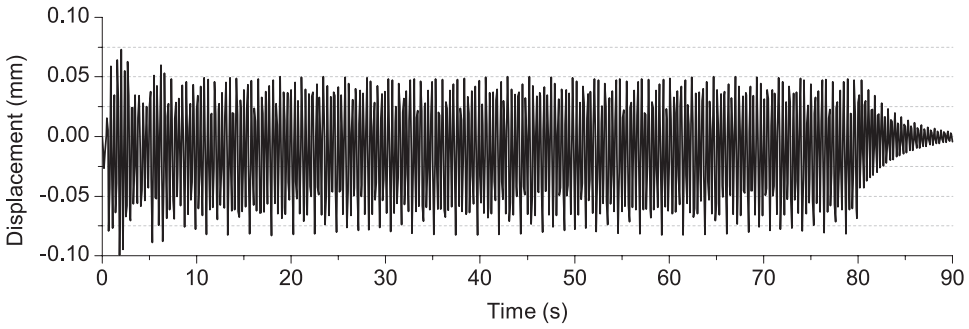

Fig. 11. Displacements of the west façade caused by the motion of bell 1.

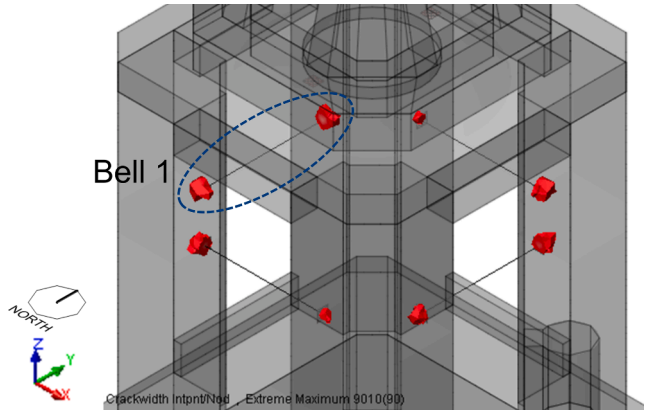

Fig. 12. Accumulative damage (in red) caused by the dynamic forces of bell 1 (crack width ranging from 0.1 to 5 μm). (For interpretation of the references to colour in this figure legend, the reader is referred to the web version of this article.)

7. Nonlinear dynamic analysis

The aim of the nonlinear dynamic analyses was to assess the influence of the bells' motion on the global response of the tower in terms of relative displacement–time history and crack pattern. For historical masonry structures, damping ratio is a sensitive parameter, which is difficult to estimate using ambient vibrations (output-only techniques) during dynamic identification tests [44]. Based on the available literature, an average value of 1.44% for all directions was adopted for the bell tower [20]. Assuming the Rayleigh viscous damping model, the upper boundary for the frequency was set to 78.45 Hz, which corresponds to 95% of cumulative participation mass in X direction and 69% in Y direction. Thus, the value calculated for proportional damping coefficients α is 0.49966 and for β is 0.00006105.

The time-varying loads used for the analyses were those actions estimated using the Runge-Kutta method, since it is faster than the analytical solution and still accurate. The time of the analyses was set to 90 s, where the excitations of the bells were applied for 80 s plus 10 s of free vibration. This time was determined by assuming a cycle in which the forces of bell 1 and bell 2 (bells with the longest periods) are in-phase (acting in the same direction) and out-of-phase (acting in opposite directions). The analyses were performed using DIANA software [45] with a time step adjusted to 0.01 s. The Hilber-Hughes-Taylor (HHT) method was applied to introduce numerical damping and cancel the numerical noise with high frequencies, which appears during the transition from the elastic to the fully cracked state of masonry [46].

7.1. Case 1: Bell 1

For this cases, only the dynamic forces of bell 1 were acting (X direction), whereas the masses of the other three bells were considered as static vertical loads. Transient response of the structure lasted less than 8 s, where the maximum displacement of 0.10 mm occurred at 1.8 s (Fig. 11). During steady-state response, the amplitude of the displacements ranged between −0.08 and 0.05 mm.

The evolution of damage was evaluated by comparing three stages: a) before the application of the dynamic loads, b) after ten seconds of loading, and c) at the end of the analysis (90 s). The crack width shown in red in Fig. 12 ranges from $1x10^{-4}$ to $5x10^{-3}$ m (0.1 to 5 μm), dimensions similar to the pores diameter of the limestone [47]. These results indicated that the numerical damage estimated in the model was quite small and thus, the masonry was hardly affected. It is worth mentioning that another analysis simulated the progressive increment of load from zero to fully magnitude of the excitation. No difference was identified between the two procedures of load application. By comparing the evolution from stage b) to c), there is no significant increment of cracks in the material.

To study the resonance, the initial angular velocity of bell 1 was increased to obtain a frequency of the predominant harmonic equal to 2.80 Hz (Section 6), which is close to the fundamental frequency of the structure in X direction (2.85 Hz). The oscillations increment was about

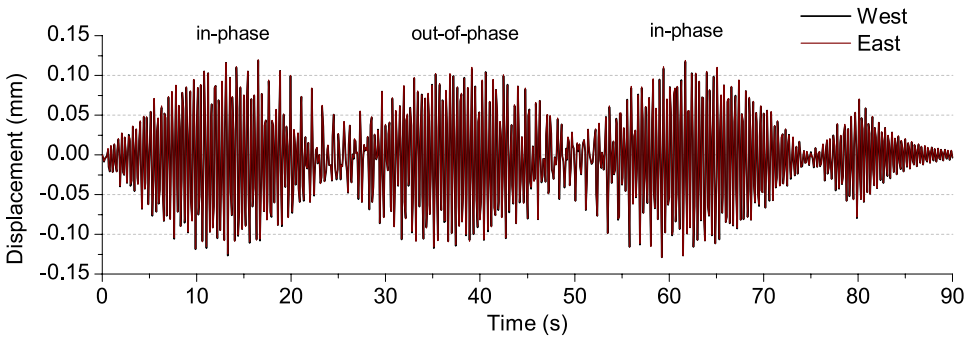

Fig. 13. Displacements of the west and east façades caused by the motion of bells 1 and 2.

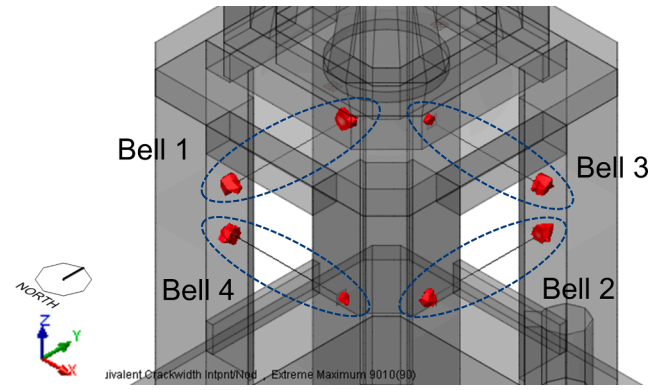

Fig. 14. Accumulative damaged caused by the dynamic forces of all the bells (crack width ranging from 0.1 to 5 μm). (For interpretation of the references to colour in this figure legend, the reader is referred to the web version of this article.)

400%, after transient response took place, the displacement amplitudes fluctuated between −0.35 to 0.30 mm in the steady-state response. Despite the significant increment of the amplitude, the results showed that the numerical damage was negligible.

7.2. Case 2: Four bells

For this case, the model was subjected to the actions of the four bells. The motion of bell 2 increased the swaying of the tower 30%, with a maximum displacement in X direction (east–west axis) of 0.13 mm in both façades. For Y direction (north–south axis), the maximum values ranged between 0.01 mm (in the north side) and 0.02 mm (in southern façade). The oscillation pattern in X direction showed that there was no transient response, and steady-state response was characterized by an amplification of the amplitude that matched the instants when the loads were in-phase and out-of-phase (Fig. 13). Such behavior is an interference phenomenon known as beat, and it is caused by the combination of two excitations of slightly different frequencies.

The motion of bell 3 and bell 4, which rotate in Y direction, does not influence the behavior of the tower in X direction. Moreover, the relative displacements measured at the height of the bells indicated that the plan section of the structure remains almost without deformation, even when the bells apply opposite forces. Fig. 14 shows that the damage in the model is insignificant, presenting crack width between 0.1 and 5 μm. The progression of damage from the beginning until the end of the load application is not important; it presents negligible increments of the cracked zones.

8. Nonlinear static analysis

A set of nonlinear pushover analyses were conducted to assess the response of the tower under two combinations of lateral loads, with the aim of determining safety levels and type of damage evaluated in terms of crack width. The horizontal and concentrated forces were applied at the center of the beams on level 6 and stepwise increased. The same control points used for the dynamic analyses were selected to plot the load capacity curves of each façade, in which the load factors are proportional to the weight of the bells.

In the first pushover analysis, the lateral response of the tower was assessed under the action of bell 1. The load was monotonically increased in the west direction (X axis). The west façade of the tower

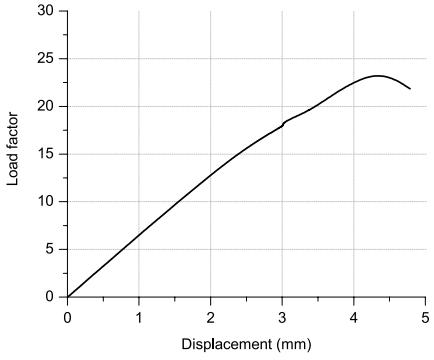

(a)

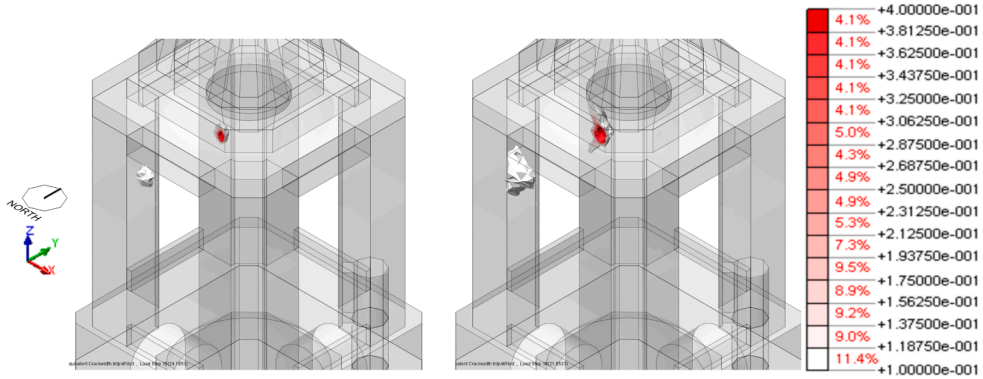

(b) (c)

Fig. 15. Results of the nonlinear pushover analysis for bell 1: a) capacity curve of the west façade, b) damage at the maximum load factor (crack width: mm), and c) damage at the maximum displacement (crack width: mm). (For interpretation of the references to colour in this figure legend, the reader is referred to the web version of this article.)

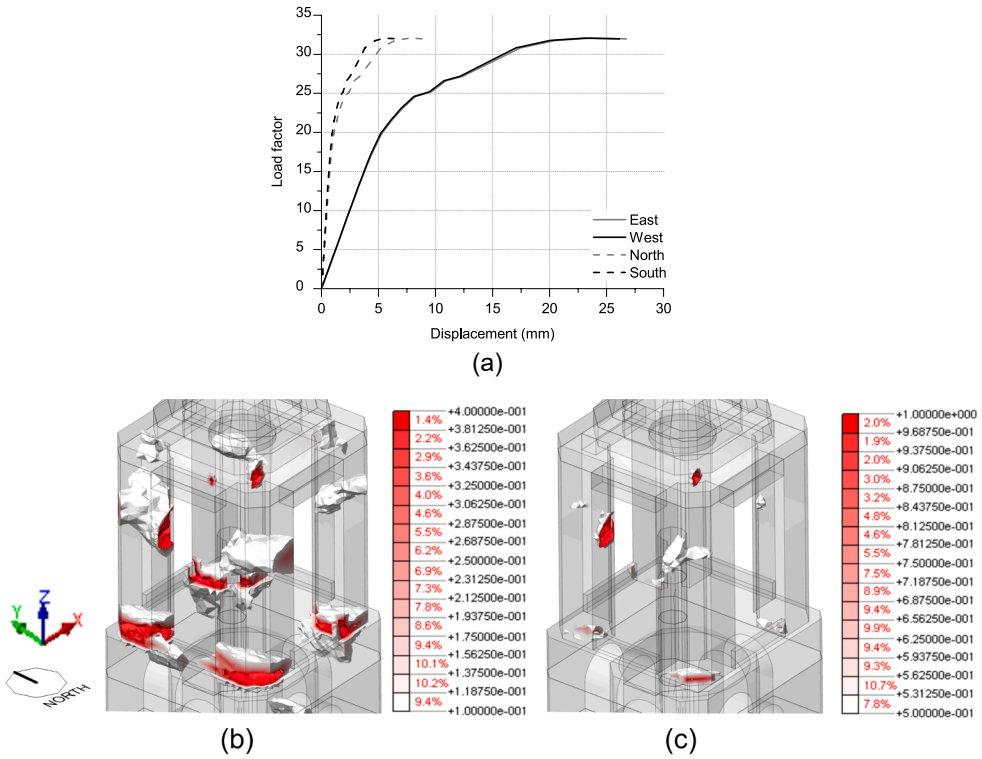

Fig. 16. Results of the nonlinear pushover analysis for the forces of the four bells applied in the same direction: a) capacity curve of the four façades, b) damage at the maximum displacement (crack width from0.1 to 0.4 mm), and c) damage at the maximum displacement (crack width from 0.5 to 1.0 mm). (For interpretation of the references to colour in this figure legend, the reader is referred to the web version of this article.)

behaved within the elastic range until a maximum load factor of 24.2, equivalent to 1,690 kN (Fig. 15a). At this point, cracks started appearing as local damage around the connections until the final failure of the masonry that occurred at the maximum displacement of 4.8 mm (Fig. 15c). Nevertheless, the stability of the piers and the global structure were not affected. Fig. 15 shows the damage at two different instants: b) at the maximum load factor (initiation of cracking) and c) at the maximum displacement (final failure).

The second pushover analysis assumed that the forces were in-phase, in which the loads of bell 1 and bell 2 were applied in + X direction (eastwards), while the loads of bell 3 and bell 4 were orientated in the + Y direction (northwards). The piers of level 6 presented the largest deformations, behaving within the elastic range until a load factor close to 20, where the first cracks appeared. The loads were increased and achieved the maximum load factor of 32 for all the bells (2235 and 1451 kN in X direction, 1080 and 699 kN in Y direction), which is associated with the maximum displacement (Fig. 16a). Local and more extensive damage was identified around the anchorage of the connections, as expected. Moreover, cracks also developed at the base of the piers, mainly in the south-west pier. The images of damage extension in Fig. 16 present different values for crack width: b) 0.1 to 0.4 mm (to compare with the previous analyses), and c) 0.5 to 1.0 mm. It should be mention that the images show the south and west façades; this allows a better visualization of the cracked zones.

9. Parametric analysis: Tower stiffness effect

Several dynamic analyses were run to evaluate the effects and influence of the stiffness of the tower and the angular velocity (increment of the dynamic forces magnitude) on the structural response. Three models with different stiffness were generated considering the tower as an isolated structure. Fundamental frequencies were used as a criteria to define the elastic properties of the models. The fundamental frequency of the calibrated model (Section 4.2) was assumed as the upper boundary (model 1), whereas the lower limit (model 3) is half of the upper boundary. The fundamental frequency of model 2 corresponds to the midpoint between upper and lower boundaries. In this procedure, one Young's modulus for the masonry was assumed for the entire tower in each model. The Young's moduli were adjusted within a realistic range to obtain the three fundamental frequencies. Table 7 presents the Young's moduli adopted for the masonry of each model and the corresponding frequency of the first mode. All the values are within the expected range of frequencies and elastic moduli presented in other masonry towers [48].

Table 7
Young's modulus and the frequency of the first mode for the three models.

	Model 1	Model 2	Model 3
Young's modulus of masonry (GPa)	23.7	11	8
Fundamental frequency (Hz)	2.87	2.15	1.47

In order to evaluate the response in terms of maximum displacements, 65 dynamic analyses were conducted assuming a linear behavior of the masonry, since no damage is expected according to the previous results. The new dynamic forces were recalculated using only the mass of bell 1. Each model was subjected to a set of excitations with different frequency content including one action with frequency equal to that of the model, aiming at studying the resonance response. The first harmonic is predominant in the majority of the dynamic forces. It should be noted that the excitations represent theoretical cases, since the respective angular velocities are not expected for bells of Spanish system.

On the left, Fig. 17a depicts the real frequencies and displacements; on the right, Fig. 17b, the frequencies were normalized (excitation frequency divided by fundamental frequency), and the dashed vertical lines represent the boundary of 10% considered in the German code DIN4178 [10]. The plots show that the admissible displacements must be under 0.5 mm for all the cases and that frequencies within the 10%

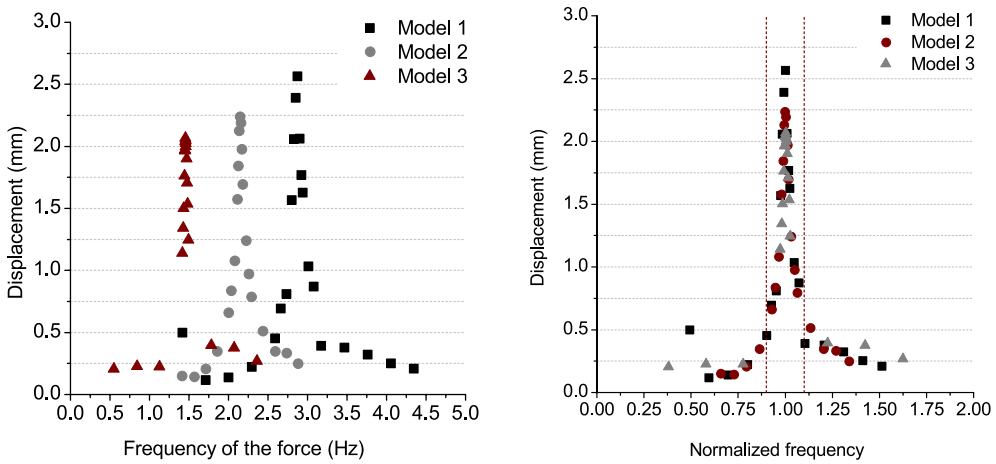

Fig. 17. Effects of the structure stiffness on the global response: (a) maximum displacements-frequency curves and (b) maximum displacements-normalized frequency curves (dashed lines represent the boundary recommended by DIN4178 [10]).

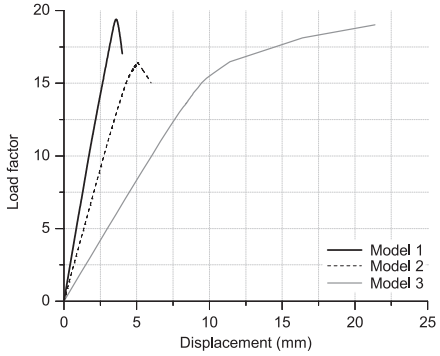

Fig. 18. Load capacity curves of the west façade of the three models when subjected to the force of bell 1.

limit increase significantly the swaying amplitude of the structure until 2.6 mm.

Along with the dynamic analyses, a nonlinear pushover analysis was performed on each model. The nonlinear properties of the masonry were the same of Table 2. The horizontal load of bell 1 was stepwise increased until achieving the maximum load capacity of the material, for which the response was evaluated through a load capacity curve (Fig. 18). The results show that the maximum load factor corresponds to Model 1, with a value of almost 20, equivalent to a force of 1,390 kN, with a quasi-brittle fracture of the material. The same fragile behavior is identified in Model 2, but associated to a load factor of 16.5 (1,150 kN). Regarding Model 3, there is hardening in the plastic response, with a maximum load factor of 19 (equal to 1,330 kN) that corresponds to the maximum deformation (21.4 mm).

Comparing these results with those obtained from the dynamic analyses of the models in terms of displacements, the amplitudes measured during resonance (maximum displacement equal to 2.6 mm) are still within the elastic range of the masonry for the three cases. Furthermore, equivalent static load factors can be identified based on the capacity curves to calculate static horizontal forces that cause the same response than dynamic actions in terms of displacements. Taking as a reference the limit point 0.5 mm, the factors ranges from 0.9 (Model 3) to 3 (Model 1).

10. Conclusions

Three methods were applied to assess the response of a masonry bell tower when subjected to excitations produced by the swinging of the bells: assessment based on frequencies, nonlinear dynamic analysis, and nonlinear static analysis. The aim was to compare the results of the three procedures based on the response of the structure. The analyses were conducted on a FEM model of the south tower of the National Palace of Mafra because of its slenderness and the location of the bells. The methodology based on frequencies and proposed in the German code DIN4178 is the simplest strategy used to assess the safety of a bell tower. It requires only two data: the frequency content of the excitation and the fundamental frequencies of the structure. Nevertheless, this approach is incapable of identifying location of damage and its severity. The frequency spectrums demonstrated that the bells of the Spanish system are also characterized by the third harmonic, and not only by the first harmonic as stated in [7].

Nonlinear dynamic analysis is the most accurate procedure to study the behavior of a structure when is affected by vibrations, although it demands a high computational effort and time. The results show that, under normal conditions, the tower behaves within the elastic range for all the cases since the dynamic actions produce small displacements. The study also reveals that the arrangement of the bells, at the central axes, avoid torsion of the tower. Additionally, nonlinear pushover analyses were also carried out aiming at determining safety levels for different load combinations. The response of the tower is linear elastic until a load factor of about 20 (20 times the weight of the bells horizontally applied). The failure of masonry consists of local damage around the connections with insignificant impact on the global stability. To cause damage, the rotation velocity needs to largely increase until values that are not possible to achieve in normal conditions.

The stiffness of the structure was also studied under forces with different magnitude and frequency content. The results show that there is an important increase in the deformation when the frequencies of the loads are within the limit of 10%, boundary stablished in the German code DIN 4178. This assessment also reveals that the maximum displacement admissible is about 0.5 mm regardless of the stiffness of the structure. Nevertheless, when comparing with the set of nonlinear pushover analysis, the three models behave linear elastic even when they are in resonance with the excitations. Furthermore, these results lead to the conclusion that, in general, linear analysis is acceptable to take into account the dynamic effects caused by bells of the Spanish system.

Finally, if crack develop close to the connections, other factors should be evaluated as source of damage, such as corrosion of the metallic pieces or masonry decay. It is also recommended to evaluate the effects of the material fatigue and creep when the bell motion is studied.

Declaration of Competing Interest

The authors declare that they have no known competing financial interests or personal relationships that could have appeared to influence the work reported in this paper.

Acknowledgements

This work was performed in the University of Minho with the funding from the ELARCH Program (Euro-Latin America partnership in natural Risk mitigation and protection of the Cultural Heritage), an Erasmus Mundus Action 2 Partnership (552129-EM-1-2014-1-IT-ERA MUNDUS-EMA21) by the European Commission and coordinated by the University of Basilicata, Italy.

References

[1] Valente M, Milani G. Seismic assessment of historical masonry towers by means of simplified approaches and standard FEM. Constr Build Mater 2016;108:74–104. https://doi.org/10.1016/j.conbuildmat.2016.01.025.
[2] Ferraioli Massimiliano, Miccoli Lorenzo, Abruzzese Donato, Mandara Alberto. Dynamic characterisation and seismic assessment of medieval masonry towers. Nat Hazards 2017;86(S2):489–515. https://doi.org/10.1007/s11069-016-2519-2.
[3] D'Ambrisi A, Mariani V, Mezzi M. Seismic assessment of a historical masonry tower with nonlinear static and dynamic analyses tuned on ambient vibration tests. Eng Struct 2012;36:210–9. https://doi.org/10.1016/j.engstruct.2011.12.009.
[4] Torelli G, D'Ayala D, Betti M, Bartoli G. Analytical and numerical seismic assessment of heritage masonry towers. vol. 18. Springer Netherlands; 2019. https://doi.org/10.1007/s10518-019-00732-y.
[5] Castellazzi Giovanni, D'Altri Antonio Maria, de Miranda Stefano, Chiozzi Andrea, Tralli Antonio. Numerical insights on the seismic behavior of a nonisolated historical masonry tower. Bull Earthq Eng 2018;16(2):933–61. https://doi.org/10.1007/s10518-017-0231-6.
[6] Milani G, Clementi F. Advanced seismic assessment of four masonry bell towers in Italy after Operation Modal Analysis (OMA) Identification. Int J Archit Herit 2019: 1–30. https://doi.org/10.1080/15583058.2019.1697768.
[7] Ivorra Salvador, Palomo María José, Verdú Gumersindo, Zasso Alberto. Dynamic forces produced by swinging bells. Meccanica 2006;41(1):47–62. https://doi.org/10.1007/s11012-005-7973-y.
[8] Ivorra S. Acciones dinámicas introducidas por las vibraciones de las campanas sobre las torres-campanario. Doctoral dissertation. Spain: Universidad Politécnica de Valencia 2002.
[9] Heyman J, Threlfall BD. Inertia forces due to bell-ringing. Int J Mech Sci 1976;18 (4):161–4. https://doi.org/10.1016/0020-7403(76)90020-5.
[10] Normung DIF. DIN 4178 Glockenturme. Germany 2005.
[11] Bru D, Ivorra S, Betti M, Adam JM, Bartoli G. Parametric dynamic interaction assessment between bells and supporting slender masonry tower. Mech Syst Signal Process 2019;129:235–49. https://doi.org/10.1016/j.ymssp.2019.04.038.
[12] Bennati S, Nardini L, Salvatore W. Dynamic behavior of a medieval masonry bell tower. Part I: Measurement and modeling of the tower motion. J Struct Eng 2005; 131:1647–55. https://doi.org/10.1061/(ASCE)0733-9445(2005)131:11(1647).
[13] Bennati S, Nardini L, Salvatore W. Dynamic behavior of a medieval masonry bell tower. Part II: Measurement and modeling of the tower motion. J Struct Eng 2005; 131:1647–55. https://doi.org/10.1061/(ASCE)0733-9445(2005)131:11(1647).
[14] Müller FP. Dynamische und statische Gesichtspunkte beim Bau von Glockentürmen. GGG I 1967;12:201–12.
[15] Wimmer A, Majer J, Niederwanger G. Dynamic behaviour and numerical simulation of old bell towers. In: Brebbia CA, editor. Struct. Repair Maint. Hist. Build. Southampton;Basel; 1989. p. 349–58.
[16] Woodhouse J, Rene JC, Hall CS, Smith LTW, King FH, McClenahan JW. The Dynamics of a Ringing Church Bell. Adv Acoust Vib 2012;2012:1–19. https://doi.org/10.1155/2012/681787.
[17] Smith R, Hunt H. Vibration of bell towers excited by bell ringing: a new approach to analysis. Leuven, Belgium: Int. Conf. Noise Vib. Eng; 2008.
[18] Wilson J, Selby A, Ross S. The dynamic behaviour of some bell towers during ringing. WIT Press 1993;4:491–500. https://doi.org/10.2495/STR930481.
[19] Selby A, Wilson J. The structural safety and acceptability of bell towers. WIT Press 1997;26:321–30. https://doi.org/10.2495/STR970311.
[20] Ivorra Salvador, Pallarés Francisco J, Adam Jose M. Masonry bell towers: dynamic considerations. Proc ICE - Struct Build 2011;164(1):3–12. https://doi.org/10.1680/stbu.9.00030.
[21] Wilson JM, Selby AR. Durham Cathedral tower vibrations during bell-ringing. Eng. a Cathedr. 1993:77–100. https://doi.org/10.1680/eac.16842.0006.
[22] Lima FMS. Analytical study of the critical behavior of the nonlinear pendulum. Am J Phys 2010;78(11):1146–51. https://doi.org/10.1119/1.3442472.
[23] Suzuki M, Suzuki IS. Physics of simple pendulum a case study of nonlinear dynamics 2008:1–60.
[24] Beléndez Augusto, Arribas Enrique, Márquez Andrés, Ortuño Manuel, Gallego Sergi. Approximate expressions for the period of a simple pendulum using a Taylor series expansion. Eur J Phys 2011;32(5):1303–10. https://doi.org/10.1088/0143-0807/32/5/018.
[25] Bakes GL, Blackburn JA. The Pendulum: a case study in physics. New York: Oxford University Press; 2005. https://doi.org/10.1063/1.2337835.
[26] Awrejcewicz J. Classical Mechanics: Dynamics. New York, Springer-Verlag New York; 2012. https://doi.org/10.1007/978-1-4614-3978-3.
[27] Boyce WE, DiPrima RC. Elementary Differential Equations and Boundary Value Problems. Seventh Ed. John Wiley & Sons, Inc.; 2001.
[28] Governo de Portugal. Sistema de Informação para o Património Arquitectónico. http://www.monumentos.gov.pt/Site/APP_PagesUser/SIPA.aspx?id=6381 (accessed August 20, 2017).
[29] Doderer G. Subsídios novos para a história dos órgãos da Basílica de Mafra. Rev Port Musicol 2002;12:87–127.
[30] Government of Portugal. General Directorate for Cultural Heritage. Royal Building of Mafra: Nomination for inscription on the World Heritage. List 2019:519.
[31] ARTeMIS. SVS, - Structural Vibration Solutions A/S. 2014.
[32] Brincker Rune, Zhang Lingmi, Andersen Palle. Modal identification of output-only systems using frequency domain decomposition. Smart Mater Struct 2001;10(3): 441–5. https://doi.org/10.1088/0964-1726/10/3/303.
[33] Midas FX+ Pre&Post-processors 2013.
[34] Karanikoloudis G, Lourenço PB. Structural assessment and seismic vulnerability of earthen historic structures. Application of sophisticated numerical and simple analytical models. Eng Struct 2018;160:488–509. https://doi.org/10.1016/j.engstruct.2017.12.023.
[35] Lourenço PB. Modelling Masonry: A Material Description. Computational Strategies for Masonry Structures. Doctoral dissertation. The Netherlands: Delft University of Technology; 1996.
[36] NTC 2018: Nuove norme tecniche per le costruzioni e Circolare n. 7 del 21 gennaio 2019 del Ministero delle Infrastrutture e dei Trasporti. Istruzioni per l'applicazione dell'«Aggiornamento delle "Norme tecniche per le costruzioni"» di cui al decreto ministeriale 17 gennaio 2018.
[37] Mendes N, Lourenço PB. Sensitivity analysis of the seismic performance of existing masonry buildings. Eng Struct 2014;80:137–46. https://doi.org/10.1016/j.engstruct.2014.09.005.
[38] Lourenço PB. Recent advances in masonry modeling: micromodelling and homogenization. In: Galvanetto U, Ferri Aliabadi MH, editors. Comput. Exp. Methods Struct. 3, Multiscale Model. Solid Mech., 2009, p. 251–94.
[39] Chopra A. Dynamics of structures.Theory and applications to earthquake engineering. Prentice Hall 2014. https://doi.org/10.1193/1.2720354.
[40] Ferraioli Massimiliano, Miccoli Lorenzo, Abruzzese Donato. Dynamic characterisation of a historic bell-tower using a sensitivity-based technique for model tuning. J Civ Struct Heal Monit 2018;8(2):253–69. https://doi.org/10.1007/s13349-018-0272-9.
[41] Palchik V, Hatzor YH. Crack damage stress as a composite function of porosity and elastic matrix stiffness in dolomites and limestones. Eng Geol 2002;63(3-4): 233–45. https://doi.org/10.1016/S0013-7952(01)00084-9.
[42] Governo de Portugal. Departamento de Estudos, Projetos, Obras e Fiscalização. Obras e Fiscalização. Palácio Nacional de Mafra. Empreitada de reabilitação dos carrilhões e das torres sineiras. Memória descritiva 2015:1–12.
[43] MathWorks. Matlab R2014a 2014.
[44] Mendes N. Seismic Assessment of Ancient Masonry Buildings: Shaking Table Tests and Numerical Analysis. Doctoral dissertation. Portugal: University of Minho; 2012.
[45] DIsplacement ANAlyzer (DIANA FEA BV), The Netherlands: TNO Building and Construction Research Institute, Delft 2018.
[46] Hilber Hans M, Hughes Thomas JR, Taylor Robert L. Improved numerical dissipation for time integration algorithms in structural dynamics. Earthq Eng Struct Dyn 1977;5(3):283–92. https://doi.org/10.1002/(ISSN)1096-984510.1002/eqe.v5:310.1002/eqe.4290050306.
[47] Figueiredo C, Folha R, Maurício A, Alves C, Aires-Barros L. Pore structure and durability of Portuguese limestones: a case study. Limestone Built Environ Present Challenges Preserv Past 2010;331(1):157–69. https://doi.org/10.1144/SP331.14.
[48] Bartoli G, Betti M, Marra AM, Monchetti S. Semiempirical Formulations for Estimating the Main Frequency of Slender Masonry Towers. J Perform Constr Facil 2017;31:1–10. https://doi.org/10.1061/(ASCE)CF.1943-5509.0001017.